Electronic Supplementary Information

The first attempt to reduce the Ni precursor $Ni(NO_3)_2$ was carried out using the method published for some metal particles supported on MIL-101(Cr) by Reich and colleagues [36], employing a microwave-assisted wet chemical method with hydrazine as the reducing agent. However, our subsequent PXRD experiments revealed that the reduction procedure also affected the MOF scaffold, as reflected in the obviously broader peaks and higher background.

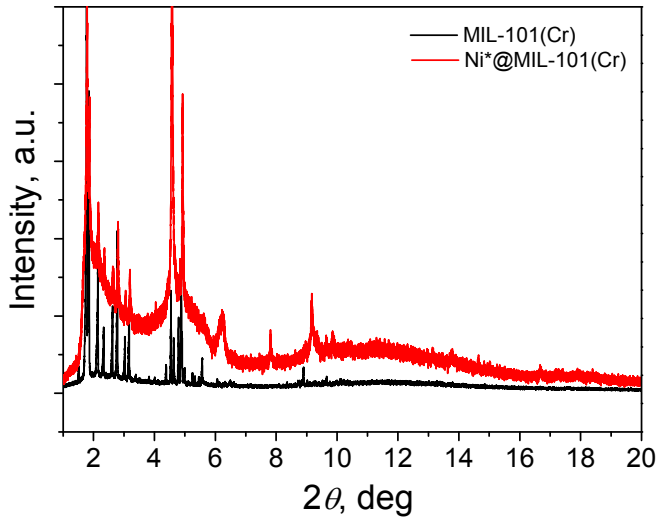

Figure S1 X-ray diffraction pattern of MIL-101(Cr) and Ni*@MIL-101(Cr) reduced by wet chemistry using hydrazine

$Ni(NO_3)_2$ was then repeated and after the heating of the sample, XPS spectra were recorded to verify the Ni oxidation state (see below). TPR experiments were carried out using hydrogen as the reducing agent in order to determine at what temperature the reduction of the nickel precursor takes place (Figure S1).

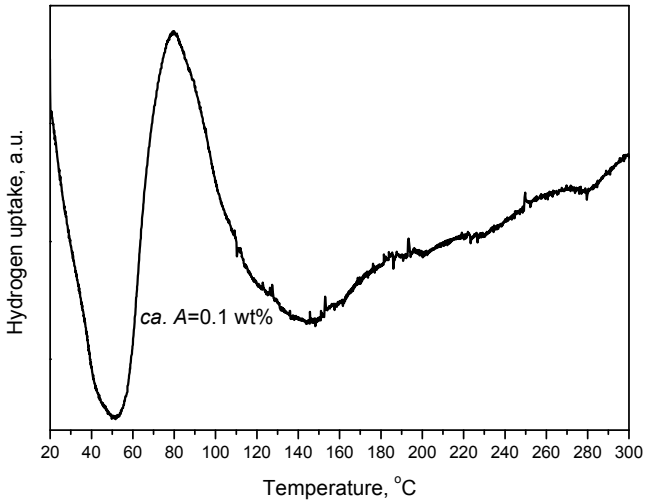

Figure S2 Temperature-programmed desorption spectrum of Ni^{2+}@MIL-101(Cr)

Following reductions of the nickel precursor were carried out at 220 °C, in a constant H_2 flow.

In Tables S2 and S3 the photo-electron binding energies are presented of Ni@MIL-101(Cr). The compositions were obtained from the sensitivity factors tabulated in [21,22]. The spectral line, analysis region and sensitivity factors are presented in Table S1 below.

Table S1 Acquisition region and area sensitivity factors are presented for the photoelectron lines analysed.

Spectral regions	Region (eV)	Sensitivity factor
C *1s*	280 – 300	0.314
O *1s*	525 – 545	0.677
Cr *2p*	570 – 600	1.623
Ni $2p_{3/2}$	845 – 895	2.309

Table S2 The composition of the sample surface of Ni@MIL-101(Cr)

Spectral line	Peak position (eV)	Area	Area fraction (%)	Sensitivity factor (area)	Atomic fraction (%)	ID
C $1s_{1/2}$	284.86	9254	79.85	0.314	41.7	aromatic C
C $1s_{1/2}$	288.62	2335	20.15	0.314	10.5	carboxyl
O $1s_{1/2}$	530.45	3349	16.11	0.677	6.1	metal oxides
O $1s_{1/2}$	531.75	13402	64.46	0.677	24.2	COO-
O $1s_{1/2}$	533.07	4040	19.43	0.677	7.3	CO_2, H_2O
Cr $2p_{3/2}$	577.33	8750	100.00	2.077	5.8	Cr(III)
Ni $2p_{3/2}$	856.42	7930	100.00	2.309	4.4	Ni(II)

Table S3 The composition of the sample surface of Ni@MIL-101(Cr) is presented and worked out for every relevant spectral line.

Spectral line	Peak position (eV)	Area	Area fraction (%)	Sensitivity factor (area)	Atomic fraction (%)	ID
C $1s_{1/2}$	284.79	4539	80.38	0.314	40.8	aromatic C
C $1s_{1/2}$	288.42	1108	19.62	0.314	10.0	carboxyl
O $1s_{1/2}$	530.43	1586	16.41	0.677	6.6	metal oxides
O $1s_{1/2}$	531.68	6302	65.22	0.677	26.3	COO-
O $1s_{1/2}$	533.05	1774	18.32	0.677	7.4	CO_2, H_2O
Cr $2p_{3/2}$	577.35	3143	100.00	2.077	4.3	Cr(III)
Ni $2p_{3/2}$	856.29	3739	100.00	2.309	4.6	Ni(II)

Identification with the X-ray Photo-electron Database of NIST shows that the metallic specimens measured are in the oxidised state of Cr(III) and Ni(II). For nickel the oxidised state is corroborated by the appearance of the shake-up peaks for both Ni 2p3/2 and Ni 2p1/2 in concert with a complete absence of photo-electron intensity at binding energies of metallic nickel. The elastic mean free path of 2p-type photo-electrons in nickel is about 1 nm what suggests that most nickel atoms are oxidised.

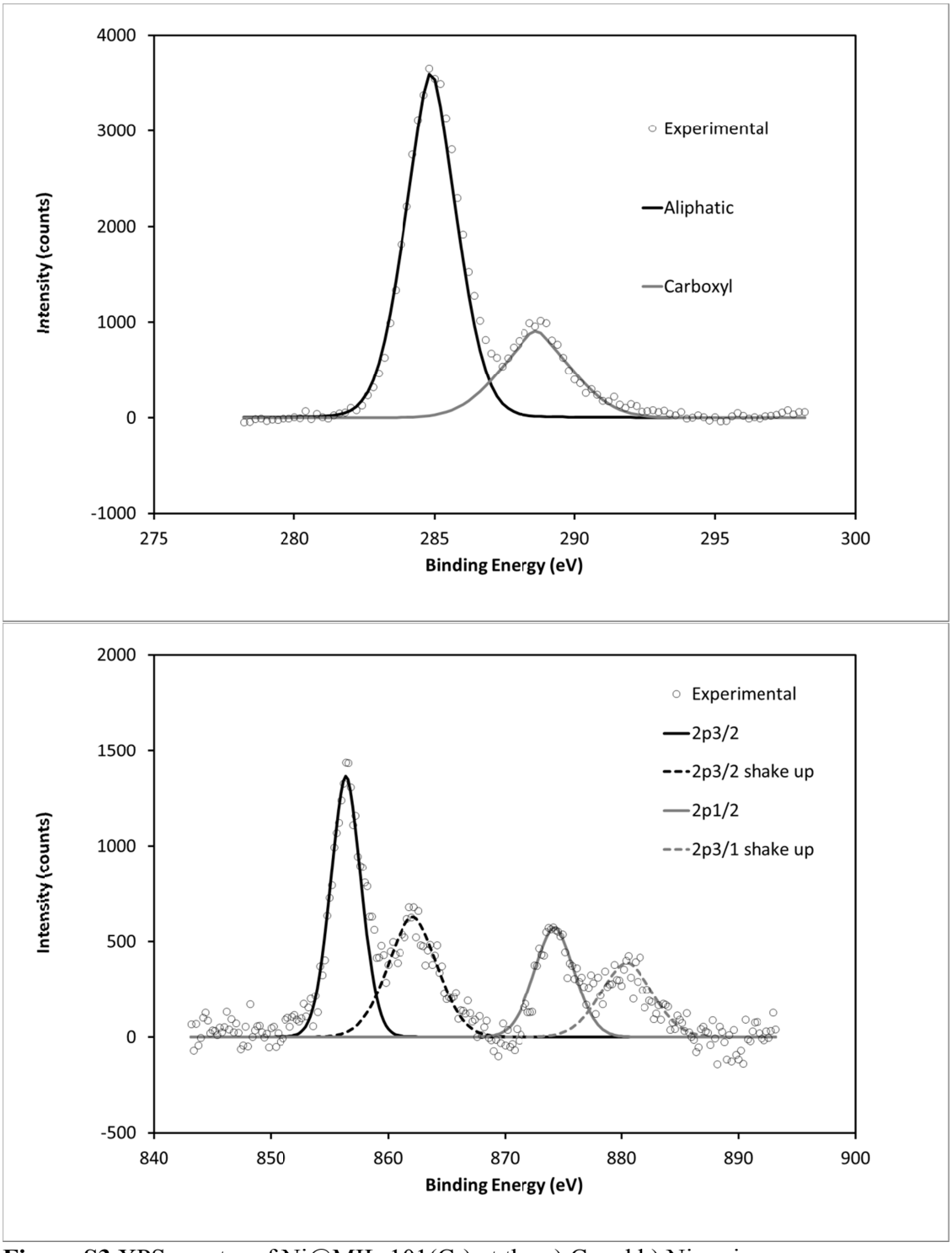

Figure S3 XPS spectra of Ni@MIL-101(Cr) at the a) C and b) Ni region.

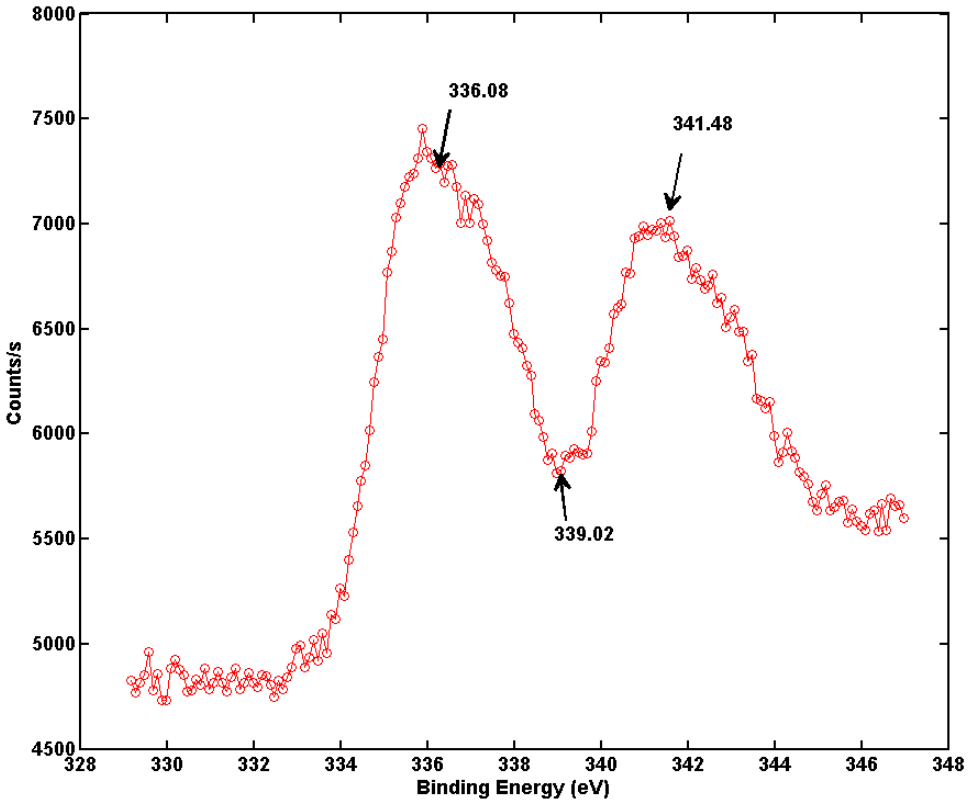

Figure S4 XPS spectrum of Pd peak in Pd/MIL-101(Cr)

FigureS4 shows a peak maximum for Pd 3d spectra at 336.08 eV and 341.48 eV, similar to what was reported previously [37,38] as complete Pd reduction. However, a careful spectrum analysis reveals that more than one state of Pd is present in the sample. On deconvolution of the peaks Pd^0, Pd^+ and Pd^{2+} states can be identified, see Table S4. Our XPS data shows that upon the exposure of the Pd@MIL-101(Cr) to air re-oxidation of the Pd particles on the MOF's surface takes place to some extent. However, the TEM evidences that the particles remained metallic in an inert atmosphere, while in the Raman spectrum of Pd@MIL-101(Cr) kept under inert atmosphere no traces of PdO and Pd_2O were observed either. This reveals that palladium nanoparticles are sensitive to air exposure to some extent, as it has been observed before. [39]

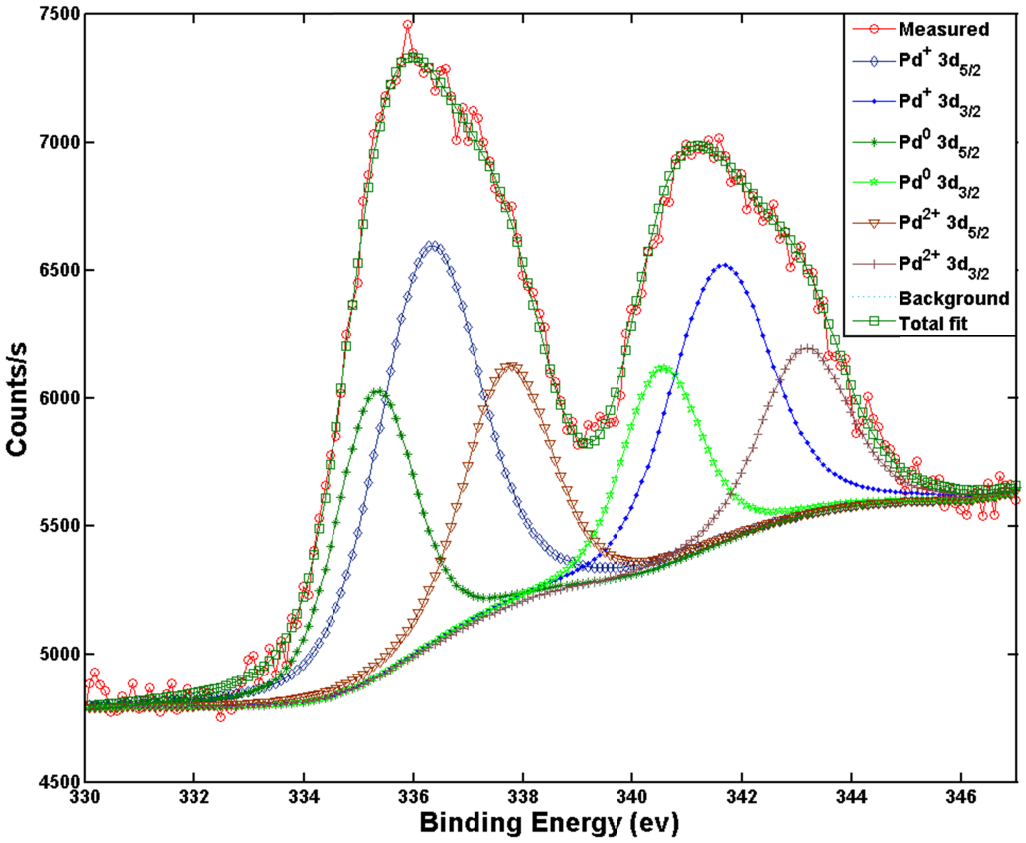

Figure S5 XPS spectrum of Pd@MIL-101(Cr) in the Pd region

Table S4 The composition of the sample surface of Pd@MIL-101(Cr)

Name	Peak BE	Height CPS	Area CPS.eV	FWHM fit parameter (eV)	L/G Mix (%) Convolve
$3d_{5/2}$ Pd^{+}	336.28	1562.79	4021.6	2.19	30
$3d_{3/2}$ Pd^{+}	341.59	1081.43	2776.44	2.19	30
$3d_{5/2}$ Pd^{0}	335.3	1121.67	2237.94	1.7	30
$3d_{3/2}$ Pd^{0}	340.52	776.18	1548.62	1.7	30
$3d_{5/2}$ Pd^{2+}	337.7	941.77	2089.17	1.89	30
$3d_{3/2}$ Pd^{2+}	343.12	651.69	1436.97	1.89	30

Table S5 BET Surface areas and total pore volumes of MIL-101(Cr), Ni@MIL-101(Cr) and Pd@MIL-101 as determined from N_2 adsorption isotherms obtained at 77 K

	BET surface area (m^2 g^{-1})	Total pore volume (cm^3 g^{-1})
MIL-101(Cr)	2231	1.079
Ni@MIL-101(Cr)	1587	1.046
Pd@MIL-101(Cr)	634	0.313

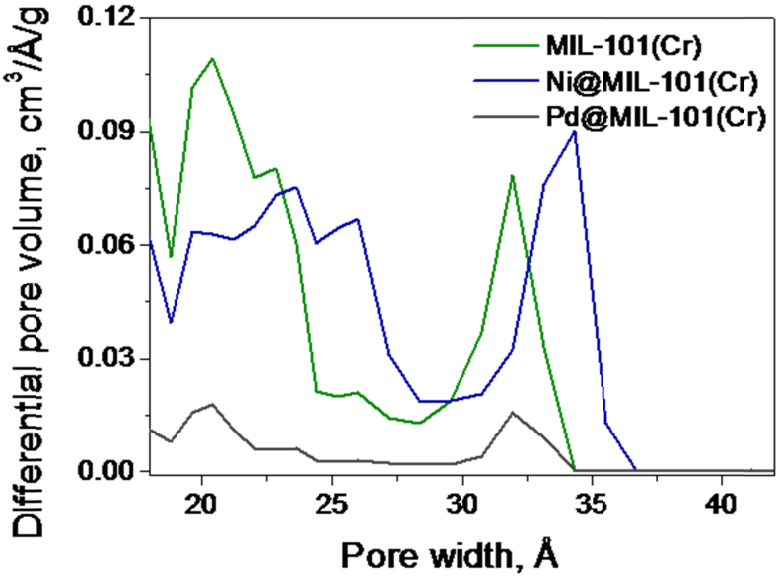

Figure S6 Pore-size distribution of MIL-101(Cr), Ni@MIL-101(Cr) and Pd@MIL-101(Cr) calculated by the DFT method.

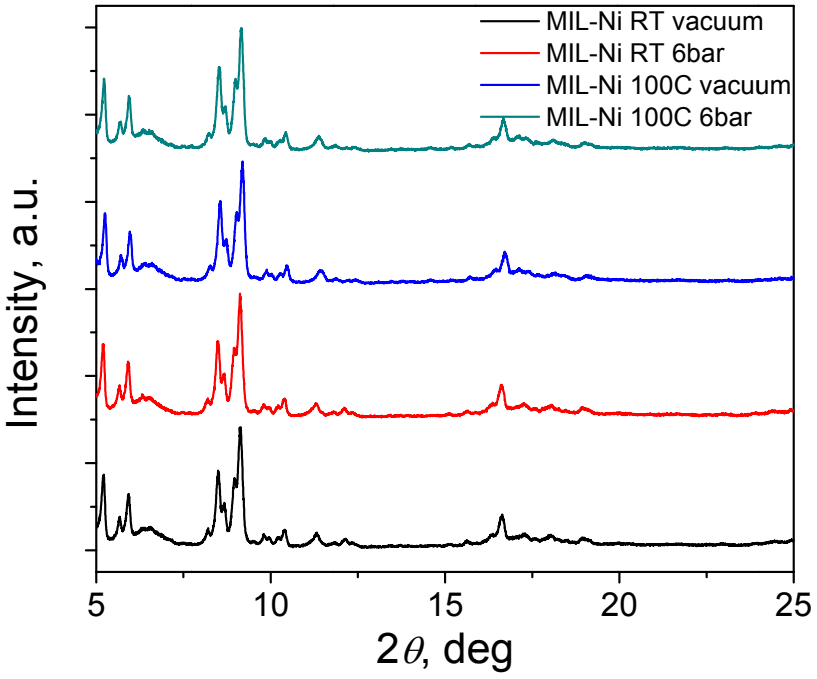

Figure S7 X-ray diffraction patterns of Ni@MIL-101(Cr) (Ni reduced in H_2 stream) at ambient temperature and at 100 °C in vacuum and under 6 bar hydrogen pressure.

Table S6 Lattice parameters of MIL-101(Cr) and Ni@MIL-101(Cr) at ambient temperature and at 100 °C in vacuum and under 6 bar hydrogen pressure (Le Bail fit)

Cell parameter ($Fd\bar{3}m$)	Ambient		100 °C	
	Vacuum	6 bar H_2	Vacuum	6 bar H_2
Pristine MIL-101(Cr)	88.681	88.802	88.753	88.753
Ni@MIL-101(Cr)	88.877	88.890	88.975	88.978

Table S7 Pd and Ni content of Pd@MIL-101 and Ni@MIL-101 as obtained by ICP analysis

	Ni content, wt%	Pd content wt%
Ni@MIL-101(Cr)	3.0	-
Pd@MIL-101(Cr)	-	7.7

References

36. M. S. El-Shall, V. Abdelsayed, A. E. R. S. Khder, H. M. A. Hassan, H. M. El-Kaderi and T. E. Reich, *J. Mater. Chem*., 2009, **19**, 7625.37.
37 Y. Huang, S. Gao, T. Liu, J. Lu¨, X. Lin, H. Li and R. Cao*, ChemPlusChem*, 2012, **77**, 106.
38. Y. Huang, Z. Lin and R. Cao, *Chem.–Eur. J*., 2011, **17**, 12706.
39. V. C. Diculescu, A.-M. Chiorcea-Paquim, O. Corduneanu and A. M. Oliveira-Brett, *J. Solid State Electrochem.*, 2007, **11**, 887.